Technical note

Bipolar implantable stimulator for long-term denervated-muscle experiments

R. G. Dennis

Institute of Gerontology, 300 N. Ingalls, Room 1056, University of Michigan, Ann Arbor, MI 48109-2007, USA

Abstract—*A micropower bipolar implantable stimulator has been developed and tested for long-term (four weeks–six months) use in experiments involving the stimulation of denervated skeletal muscle. Implantable stimulators are typically operated from a single lithium battery at 3 V. After the first week of denervation, stimulation of denervated muscles of rats requires voltages in the range of 6–12 V. The stimulator described can deliver voltages up to 15 V, with variable pulsewidth, frequency and duty cycle. All stimulation parameters are set prior to implantation by selection of appropriate resistors and capacitors. Each primary failure mode for implantable stimulators is addressed. Long-term reliability rates in excess of 95% are achievable if the construction details are followed closely. Methods for battery power management, circuit component selection, electrode construction and encapsulation are described in detail. This device is not intended for use in humans.*

Keywords—*Implantable, Stimulator, Chronic stimulation, Muscle stimulation, Denervated muscle, Muscle*

Med. Biol. Eng. Comput., 1998, **36**, 225–228

1 Introduction

A NUMBER of implantable electronic stimulators have been developed recently for scientific and clinical applications, such as conditioning skeletal muscle for use in cardiac assist devices and studying the effects of chronic and intermittent stimulation on contractile properties and fibre type transformation.

The implantable muscle stimulators reported previously have been intended for stimulation of muscles with nerves intact (SALMONS, 1966; BROWN and SALMONS, 1981; COOPER and SALMONS, 1988; JARVIS and SALMONS, 1991; SALMONS and JARVIS, 1991; SMITH, 1978; WILLIAMS and HERBERT, 1985). These stimulators are inadequately powered for fully stimulating denervated muscle (MACPHERSON *et al.*, 1997).

In rats, denervation results in a loss of the specific force capacity of limb muscles of approximately 95% within four–eight weeks (unpublished data), and therefore an implantable stimulator must be capable of providing adequate stimulation for at least eight weeks. Stimulation of denervated muscle has generally been performed by tethering the animals and stimulating with transcutaneous electrodes (ROSENBLATT *et al.*, 1987; 1989), which presents logistical problems of housing and caring for the animals. The use of fully implantable devices is desirable for experiments on the long-term effects of electrical stimulation on denervated muscle.

Problems with existing implantable stimulator designs include a high failure rate, often around 30% (SALMONS and JARVIS, 1991), due to leakage or electrode failure, electrochemical damage to tissue (GUYTON, 1974) and limited battery life. The electrode failure modes include electrode breakage due to cyclic mechanical loading and fatigue from activity of the animals, and electrochemical degradation of the electrode tip. The present design addresses each of these issues. The total cost of each unit is less than US $50, and the circuits can be reused by peeling away the encapsulant, replacing the battery and electrode wires, and re-encapsulating the device.

2 Circuit description

The stimulator uses 4000 series CMOS integrated circuits and logic-level FET transisitors (Fig. 1). Surface mount components are used to minimise size (Fig. 2). The logic is operated at battery voltage, represented as 3 V on the schematic diagram. The actual battery voltage will range from 2.65 to 2.9 V, depending upon the type of lithium battery used. The stimulator provides bipolar pulses by alternately discharging a capacitor (C_4) through first one, then the other, electrode. The capacitor is trickle charged through R_4 to a voltage that is set by the number of 3 V lithium batteries that are stacked in series, up to a maximum voltage of 15 V. The logic circuit is powered from the battery at the negative end of the battery stack.

Bipolar operation is necessary to eliminate the generation of gases at the electrodes by electrochemical dissociation of water, as well as to prevent anodic degradation of the metal electrode surface. Capacitive discharge to the electrodes is employed to allow the logic circuit to be operated at 3 V, while stimulating at any voltage up to 15 V, to increase

Correspondence should be addressed to Dr Dennis.

First received 5 August 1997 and in final form 20 October 1997

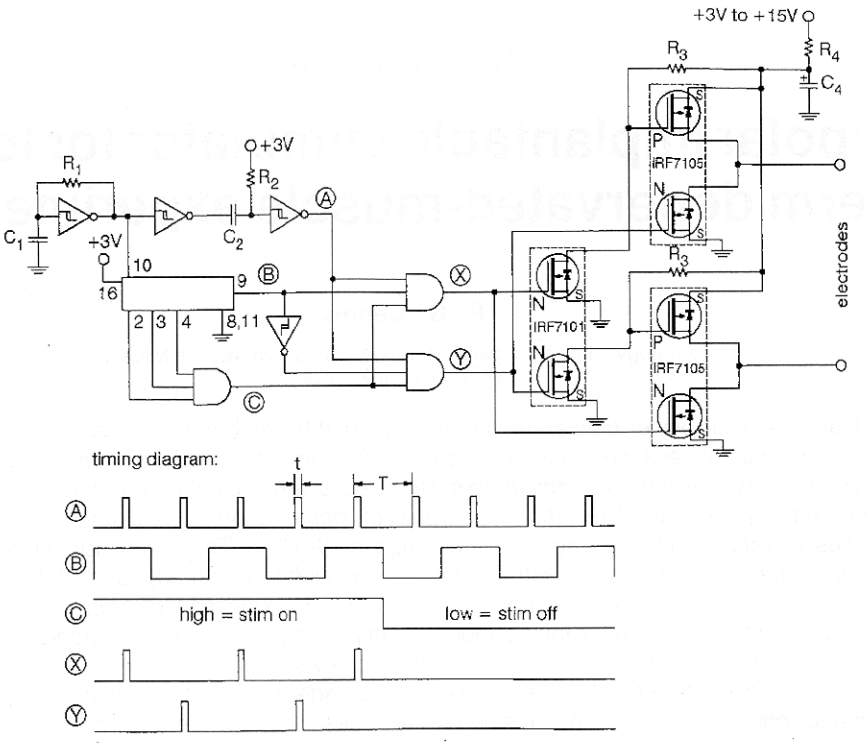

Fig. 1 *Schematic diagram of bipolar capacitive discharge implantable stimulator. All integrated circuits are 4000 series CMOS to minimise power consumption and to allow operation at 2.7 to 3.0 V, and are SOIC package size. The 12-bit counter is a National Semiconductor CD4040B, Motorola MC14040B, or Philips HEF4040B. The hex inverter is a National Semiconductor CD40106B, Motorola MC14106B, or Philips HEF40106B. The three- input AND is a National Semiconductor CD4073B, or Motorola MC14073B. The dual n-channel HEXFET is an International Rectifier IRF7101 in an SO-8 package. The dual n and p-channel HEXFETs are International Rectifier IRF7105 or IRF7106, in an SO-8 package. All passive components are SMD package size 0805. Resistors are 5% tolerance, capacitors are 10% tolerance. R_3 is 1 MΩ (at both locations), R_4 is 10 kΩ, and C_4 is Panasonic type EF 2.2 μF, 16 V, resin-dipped tantalum. R_1 and C_1 set the clock frequency (eq. 1), and R_2 and C_2 set the pulsewidth (eqn. 2). C_3 is optional (not shown), and is a 0.1 μF capacitor across the +3 V and ground rails to stabilise the 3 V supply*

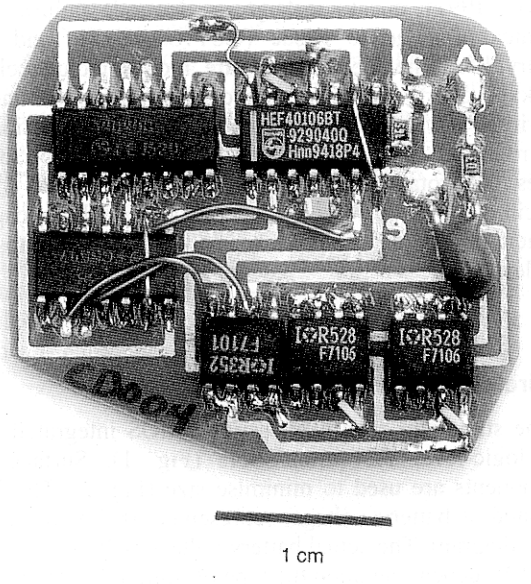

Fig. 2 *Completed circuit prior to encapsulation. Batteries and electrode wires are not shown. The construction uses 0805 size surface mount resistors and capacitors, and standard surface mount integrated circuits (SOIC). The substrate is 1.4 mm (0.055 in) thick phenolic with copper cladding. The electrode wire is Cooner Wire P/N: AS633, 0.33 mm (0.13 in) outer diameter stranded stainless steel electrode wire with TFE insulation*

current output by reducing the output impedance of the device, and to extend battery life by reducing the peak current drain from the battery.

3 Calibration

Values for the stimulator frequency f and pulsewidth t are set by the passive components R_1, C_1, R_2 and C_2 (Fig. 1, eqns. 1 and 2). High resistance values and low capacitance values are used for passive components to minimise the unloaded current drain. Resistors in the range of 1.0–5.0 MΩ are optimum. The low-power oscillator and digital differentiator are implemented using inverter gates with hysteresis bands, which vary from manufacturer to manufacturer and lot to lot so the actual resistor and capacitor values must be selected by trial and error. The values of R_1 and C_1 set the oscillator frequency, estimated by

$$f = \frac{1}{T} = \frac{1}{0.8R_1C_1} \tag{1}$$

where f is the clock frequency (Hz) and T is the clock period (s). The resulting frequency is measured at test point A (Fig. 1), and the coefficient 0.8 is modified as necessary. The values of C_2 and R_2 set the pulsewidth t (s) approximately:

$$t = 1.2R_2C_2 \tag{2}$$

With no load on the electrodes and operating with a 25 Hz continuous output frequency at a pulse width of 200 μs, the unloaded operating current is related to the supply voltage as

$$I_u = 11V^2 - 49V + 58 \quad \text{for} \quad 2.2 < V < 6.0 \tag{3}$$

where I_u is the operating current (μA) with no load on the electrodes, and V is the supply voltage. Note that a supply voltage of 2.80 V results in a supply current of only 7 μA, whereas a supply voltage of 5.00 V results in a supply current

of 88 μA. Micropower oscillators of this type should be operated at the lowest possible voltage (< 3 V), to avoid the large class A current due to rail-to-rail conduction during the period that the oscillator is operated near the CMOS threshold (HOROWITZ and HILL, 1989). The unloaded current drain is also proportional to clock frequency. If a frequency other than 25 Hz is used, the result of eqn. 3 is multiplied by the ratio $f/25$, to determine I_u.

Variations in the supply voltage influence the clock frequency and pulsewidth. The device is calibrated at the stable operating voltage of the lithium battery, generally in the range of 2.70 V–2.90 V, because the stimulator circuit is powered by an unregulated voltage source. In general, calibration at 2.80 V is adequate to ensure an accuracy of stimulation parameters within ±5%. The stable operating voltage is determined by applying a load of 10 kΩ to the battery for three days. The clock frequency and pulsewidth are each influenced by the supply voltage as follows:

$$f/f_c = 0.34V + 0.04 \quad \text{for} \quad 2.5 < V < 3.2 \tag{4}$$

$$t/t_c = -0.33V + 1.94 \quad \text{for} \quad 2.5 < V < 3.2 \tag{5}$$

where f is the clock frequency, t is the pulse width, V is the actual supply voltage, and f_c and t_c are the calibrated clock frequency and pulsewidth at the calibration voltage of 2.80 V.

The duty cycle is set by connecting the three inputs of the AND gate near test point C to counter outputs as shown, or by tying them to +3 V (Fig. 1). Stimulation is enabled when all three inputs are logic HIGH, and thus a duty cycle of 100, 50, 25 or 12.5% can be selected. The connections shown in Fig. 1 result in a 12.5% duty cycle, in which case the repeating stimulation pattern is stimulation ON for 16 clock pulses, and OFF for the following 112 clock pulses. A 100% duty cycle is selected by tying all three inputs to +3 V. Unused counter outputs must be left unconnected, and all unused logic inputs must be tied to ground or +3 V.

4 Battery life

Batteries are rated for voltage and capacity in milliAmp hours (mAh) for a fixed load. The product of voltage and mAh capacity is the total energy content of the battery. The actual capacity of a battery depends upon the service conditions. Lithium batteries are sensitive to excessive current drain, and the actual capacity of the battery is a function of the peak current drain when the load on the battery varies periodically, as in the case of chronic stimulation. Peak current and average current to the capacitor C_4 can be determined by placing electrodes in the muscle and measuring the voltage V_{R_4} across R_4, through which the discharge capacitor C_4 is charged (Fig. 1). The peak current drain from the battery during stimulation will occur at the end of each pulse

$$I_{peak} = (10^6 * V_{maxR_4}/R_4) + I_u \tag{6}$$

where I_{peak} is in μA, and V_{maxR_4} is the maximum voltage drop across R_4, which occurs at the end of each stimulus pulse. The estimated capacity for small lithium batteries (25–250 mAh rated capacity) is

$$Q = (-0.22 \ \ln(I_{peak}/1000) + 0.64)K \tag{7}$$

where Q is the estimated capacity (mAh), and K is the manufacturer-specified battery capacity (mAh). For example, a lithium battery rated at 48 mAh, but subjected to a load with a peak current of 1000 μA, would only provide 64% of the rated capacity, or 31 mAh. This equation assumes that the battery has failed when the operating voltage drops to 90% of the stable operating voltage, and provides a more conservative estimate for larger-capacity lithium batteries.

The typical impedance of both denervated and innervated rat skeletal muscle is 1500 Ω for 2 mm-long needle electrodes inserted into the muscle belly at a longitudinal separation of 8 mm (MACPHERSON *et al.*, 1997). This impedance value should be verified for the specific electrode configuration employed. The average current drain through the electrodes is

$$I_e = 10^6 * (V_s/1500) tN \tag{8}$$

where I_e is in μA, V_s is the total voltage of the battery stack that charges the capacitor C_4, t is the pulsewidth in seconds, and N is the average number of pulses per second, taking into account the fact that the duty cycle may be set to less than 100%. Capacitor leakage I_L (μA) is

$$I_L = 0.02 \ V_s \tag{9}$$

The average current drain I_{avg} (μA) on the battery when the stimulator is implanted is

$$I_{avg} = I_u + I_e + I_L \tag{10}$$

The operational life expectancy L of the implantable stimulators is

$$L = \frac{1000 \cdot Q}{I_{avg}} \tag{11}$$

where L is measured in hours, Q is the battery capacity in mAh (eqn. 7), and I_{avg} is the average current consumption, in μA, of the stimulator when implanted. For the preceding equations, eqns. 1–8 result from experimental data with best fit curves, eqn. 9 is the published leakage rate for Panasonic tantalum capacitors (Fig. 2), eqn. 10 is the sum of all sources of current drain (eqns. 3, 8 and 9), and eqn. 11 is the actual battery capacity (mAh) divided by average current drain (mA), with a multiplicative factor to express the expected battery life in units of hours. Final battery capacity for the device is selected on the basis of the calculations of the anticipated battery life as well as the general guideline that the total mass of the implanted device should not exceed 5% of the body mass of the animal.

5 Electrodes

The electrode wire is 36 AWG stranded, TFE coated wire*. Electrode wires are cut to a length that is approximately 100 mm longer than needed, to allow the wires to be folded back within the encapsulation to reduce the likelihood of leakage. Improper soldering of the stainless-steel electrode wires invariably results in device failure due to corrosion or solder-joint failure. A good solder joint with the stainless-steel electrode wire is formed by touching a bead of molten solder to a 1 mm stripped end of electrode wire that is immersed in a small drop of zinc chloride soldering flux. The instant that the flux evaporates, the solder will wick onto the stainless-steel wire. The tinned electrode ends are cleaned with soap and warm water to remove flux. The free ends of the electrode wires remain unstripped until ready for implantation, to avoid the possibility of inadvertently shorting the device and reducing the battery life. Immediately prior to implantation, 1–2 mm of insulation is stripped from the end of each electrode wire.

* Available from Cooner Wire Co.

6 Encapsulation

Acceptable encapsulant materials that have been tested include Dow Corning #732 or Dow Corning #734 clear RTV silicone sealant (DONALDSON, 1989). Neither of these substances is accepted for implantable devices intended for human use. The silicone sealant is initially mixed with an equal volume of toluene, and toluene or sealant is added as necessary to achieve the consistency of thin syrup. Air bubbles are removed by subjecting the encapsulant mixture, in an open container, to a partial vacuum of 68 kPa for 2 min, followed by 85–92 kPa for approximately 5 min. To test for proper viscosity, a 5 cm^3 syringe (do not substitute sizes) is used as a makeshift Saybolt viscometer. The needle is removed from the Luer taper, and the syringe is filled entirely, with the plunger removed. The open-topped syringe is held vertically to time the rate at which the encapsulant drains from the 5 cm^3 to the 4 cm^3 mark. The viscosity is adjusted until the drain time is 20–30 s. The encapsulant mixture can be stored for up to six months in a wide-mouthed glass container with a Teflon™ seal and tight-fitting cap.

The stimulators are hung by the electrode wires for conformal coating and during the encapsulation process. Prior to encapsulation, two conformal coats are applied to protect the circuit from the acetic acid in the sealant. A silicon resin-type conformal coat† is used in the construction of these devices. The stimulator is dipped into the encapsulant mixture exactly as a candle wick is dipped into hot wax. Each encapsulant coating is allowed to dry for 1.5–2 h before additional coats are applied. Voids in the coating are filled by injecting encapsulant with a 1 cm^2 syringe. A total of four coats are applied and allowed to dry overnight.

The electrode wires are folded back across the batteries, and each is pulled through the small drop of hardened silicon encapsulant at the bottom of the stimulator using number 5 forceps‡. The electrode wire is wound tightly around an 18 gauge needle for five or six turns to create a tight helix of wire directly adjacent to the stimulator body. An additional five–seven coats of encapsulant are applied. The encapsulant forms a tapering cone on the electrode wire that extends about 3 cm from the stimulator body and reaches a maximum diameter of about 3 mm closest to the stimulator body. This acts as a strain relief to minimise wire breakage or leakage into the stimulator electronics along the electrode wires. The encapsulant is allowed to dry for a full week before implantation. A load of 1.0–2.2 kΩ is placed across the electrodes for verification of function once the device has been encapsulated.

7 Conclusions

The circuit design and construction methods described here allow the stimulation of denervated limb muscles in rats with an implantable device for periods of up to six months. The described methods of construction and calibration result in a device that has vastly reduced failure rate due to electrochemical degradation of the electrode tips, leakage or unanticipated battery failure.

Acknowledgements—The author would like to thank Dr. Peter Macpherson for assistance with the muscle impedance testing, and Richard Hinkle and Cheryl Hassett for assistance with stimulator implantation and evaluation.

This work was supported by the National Institute on Aging Grant AG-10821.

References

BROWN, J. and SALMONS, S. (1981): 'Percutaneous control of an implantable muscle stimulator via an optical link', *J. Biomed. Eng.*, **3**, pp. 206–208

COOPER, J. P. and SALMONS, S. (1988): 'A simple three-program implantable muscle stimulator with optical control', *J. Biomed. Eng.*, **10**, pp. 467–469

DONALDSON, P. E. K. (1989): 'Encapsulating microelectronic implants in one-part silicone rubbers', *Med. Biol. Eng. Comput.*, **27**, pp. 93–94

GUYTON, D. L. (1974): 'Theory and design of capacitor electrodes for chronic stimulation', *Med. Biol. Eng.* (Sept.), pp. 613–620

HOROWITZ, P. and HILL, W. (1989): 'The art of electronics' (Cambridge University Press) pp. 967–968

JARVIS, J. C. and SALMONS, S. (1991): 'A family of neuromuscular stimulators with optical transcutaneous control', *J. Med. Eng. & Tech.*, **15**, (2), pp. 53–57

MACPHERSON, P. C. D., DENNIS, R. G. and FAULKNER, J. A. (1997): 'Changes in impedance and excitability of soleus muscles from rats after 4 weeks of denervation', *FASEB J.*, **11**, p. A56

ROSENBLATT, J. D., LIN, P. J., MCKEE, N. H. and PLYLEY, M. J. (1987): 'A simple method for concurrent stimulation of skeletal muscle in several animals', *Can. J. Sport Sci.*, **12**, p. 20P

ROSENBLATT, J. D., LIN, P. J., MCKEE, N. H. and KUZON, W. M. Jr (1989): 'A simple method for the concurrent stimulation of skeletal muscle in several animals', *Lab. Animal Sci.*, **39**, (4), pp. 347–348

SALMONS, S. (1966): 'An implantable muscle stimulator', *J. Physiol.*, **188**, pp. 13–14P

SALMONS, S. and JARVIS, J. C. (1991): 'Simple optical switch for implantable devices', *Med. Biol. Eng. Comput.*, **29**, pp. 554–556.

SMITH, D. M. (1978): 'Miniature stimulator for chronic animals', *Pflugers Arch.*, **376**, pp. 93–95

WILLIAMS, G. F. and HERBERT, M. A. (1985): 'Totally implantable muscle stimulator with automatic daily cycling', *Med. Biol. Eng. Comput.*, **23**, pp. 601–603

† Chemtronics Konform SR 2000.

‡ Fine Science Tools.